INSTITUTO SUPERIOR TÉCNICO

PROJECTO MEFT

Linearized General Relativity in Hyperboloidal Coordinates

Author:
Filipe Ficalho

Supervisor:
Prof. David Hilditch

Research work performed for the Master in Physics Engineering

at

GRIT
CENTRA

January 8, 2025

1 Introduction

When studying gravitational waves, one has to keep in mind that gravitational wave sources (like black hole mergers, neutron stars, etc.) are usually located billions of light years away from us. From the point of view of an observer on Earth, this distance is so vast that it can be approximated as being at infinity. This distance, however, is not sufficiently far away to require accounting for the cosmological constant, allowing us to model spacetime as asymptotically flat. Thus, we are interested in studying the behavior of the gravitational fields at null infinity, $\mathscr{I}$.

To do so, we must perform a conformal compactification of the spacetime, which brings $\mathscr{I}$ to a finite distance on our computational grid. This is done by working in the hyperboloidal coordinate system.

1.1 Hyperboloidal Coordinates

The hyperboloidal coordinate system, as previously mentioned, maps our previously unbonded domain to a finite one. This is done by introducing new time and radial coordinates (t, r), which are related to the spherical coordinates of Minkowski spacetime (T, R) by the transformations

$$t = T - H(R) \quad R = \frac{r}{\Omega(r)} \,, \tag{1}$$

where $H(R)$ is called the height function and $\Omega(r)$ is called the compress function, which give rize to the following Jacobian matrix:

$$\left(J^{Hyp}\right)_{\alpha'}^{\ \beta} = \begin{pmatrix} 1 & -H'(r) & 0 & 0 \\ 0 & \frac{L(r)}{\Omega^2(r)} & 0 & 0 \\ 0 & 0 & 1 & 0 \\ 0 & 0 & 0 & 1 \end{pmatrix} \,, \tag{2}$$

where $H'(r)$ denotes the derivative of the height function with respect to R written as a function of r, and $L(r)$ is defined as

$$L(r) \equiv \Omega(r) - r\,\partial_r \Omega(r) \,. \tag{3}$$

This coordinate system is particularly useful because it is possible for us to choose the height and compress functions in such a way that the outgoing light speed is constant. This however has the tradeoff of making the incoming light speed decrease as it reaches $\mathscr{I}$. This property can be observed in figure 1 for a specific choice of the height and compress functions.

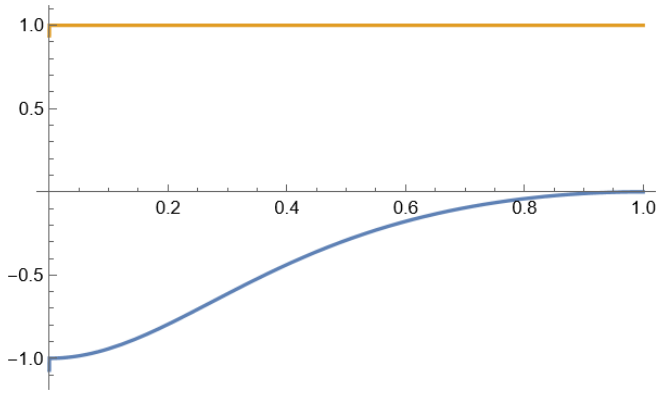

FIGURE 1: Outgoing and incoming light speeds for $H(R) = \frac{2R^2+S^2-\sqrt{4R^2S^2+S^4}}{2R}$ and $\Omega(r) = 1 - \frac{r^2}{S^2}$, with $S = 1$.

Throughout this work, we will sacrifice this very relevant property in exchange for ease of manipulation of the expressions, since the goal of this introductory work to the subject is to get accostumed with the coordinate system. The height and compress functions that will used throughout this work are

$$H(R) = \sqrt{S^2 + R^2} \quad \Omega(r) = \frac{1}{2}\left(1 - \frac{r^2}{S^2}\right) \quad , \tag{4}$$

where S is a constant that determines the size of the compactified domain. The choice of S is arbitrary, as it simply defines what point $\mathscr{I}$ will be maped to. We will set $S = 1$. As a consequence of our previous choices, we also have

$$H'(r) = \frac{2rS}{S^2+r^2} \quad L(r) = \frac{1}{2}\left(1 + \frac{r^2}{S^2}\right) . \tag{5}$$

For this choice of functions, we still have that the incoming light speed decreases as it reaches $\mathscr{I}$. However, we don't have a constant outgoing propagation speed. This can be seen in figure 2. The only implication this choice will have in our results is that the wave will take longer to reach $\mathscr{I}$ and will be slightly distorted. This is not a problem for our purposes, since on this first approach we are only interested in making sure the code converges smoothly towards the solution.

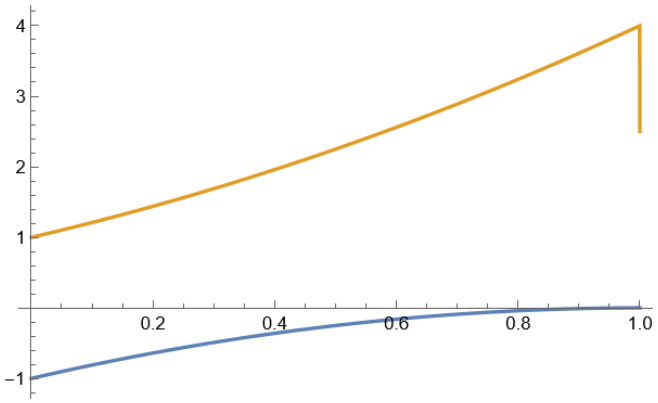

FIGURE 2: Outgoing and incoming light speeds for $H(R) = \sqrt{S^2 + R^2}$ and $\Omega(r) = \frac{1}{2}\left(1 - \frac{r^2}{S^2}\right)$, with $S = 1$.

1.2 Computational Setup

This work is a continuation of my previous work on numerical relativity. As such, the framework used here is the same as the one used in that work, with the adition of truncation error matching for the derivatives, interpolation at the boundaries and the Evans Method for regularization at the origin. The description of the base code can be found in [], and this section will elaborate on the upgrades made.

1.2.1 Truncation Error Matching

Truncation error matching is a technique used to improve the accuracy of the numerical solution by matching the truncation error of the finite difference scheme used on the boundaries to the truncation error of the one used in the interior of our computational domain. This is done by using a one sided finite difference scheme on the boundaries such that the leading order error term is the same as the one used in the interior.

In our framework, we use the following second order finite difference scheme for the first derivative of a field ψ at an interior point i (where the leading order error term was written explicitly):

$$\psi_i' = \frac{\psi_{i+1} - \psi_{i-1}}{2h} - \frac{h^2}{6}\psi_i''' + \dots , \tag{6}$$

where ψ_{i+1} and ψ_{i-1} are the values of the field ψ at the points $i+1$ and $i-1$ respectively, and h is the grid spacing.

To match this leading order term of the error, we use the following one sided finite difference scheme for the derivative of f at the left and right boundary points respectively []:

$$\psi_i' = \frac{\psi_{i+3} - 4\psi_{i+2} + 7\psi_{i+1} - 4\psi_i}{2h} - \frac{h^2}{6}\psi_i''' + \dots \tag{7}$$

$$\psi_i' = \frac{4\psi_i - 7\psi_{i-1} + 4\psi_{i-2} - \psi_{i-3}}{2h} - \frac{h^2}{6}\psi_i''' + \dots \tag{8}$$

1.2.2 Interpolation at the Boundaries

Since we are interested in evolving the fields at null infinity, we must choose a boundary condition that allows the fields to freely propagate outwards. To do so, we use interpolation at the outer boundaries of our computational domain to fill the ghost points in those regions. This is done by using the following interpolation scheme:

$$\psi_i = 4\psi_{i-1} - 6\psi_{i-2} + 4\psi_{i-3} - \psi_{i-4} , \tag{9}$$

where ψ_i is the value of the field at the ghost point i, and ψ_{i-1}, ψ_{i-2}, ψ_{i-3} and ψ_{i-4} are the values of the field at the points $i-1$, $i-2$, $i-3$ and $i-4$ respectively.

1.2.3 Evans Method

When dealing with operators like the Laplacian in spherical coordinates, we find some formal singularities which need to be removed in order for our code to work. To remove those singularities, we can apply the Evans Method. This method consists of rewriting the singular terms as a different differential operator, called the Evans operator, which can be evaluated at the grid points. The Evans operator is defined as

$$\partial_r\psi + \frac{p}{r}\psi = (p+1)\frac{d(r^p\psi)}{dr^{p+1}} , \tag{10}$$

where p is a constant. This operator can be expressed in terms of the grid points as

$$(p+1)\frac{d(r^p\psi)}{dr^{p+1}} = (\tilde{D}\psi)_i = (p+1)\frac{r_{i+1}^p\psi_{i+1} - r_{i-1}^p\psi_{i-1}}{r_{i+1}^{p+1} - r_{i-1}^{p+1}} , \tag{11}$$

where the subscripts $i+1$ and $i-1$ denote the grid points $i+1$ and $i-1$ respectively.

2 Wave Equation in 1+1 Dimensions

We start by considering the wave equation in 1+1 dimensions

$$\Box\psi \equiv -\partial_T^2\psi + \partial_X^2\psi = 0 . \tag{12}$$

From my previous work on the subject [], we concluded that we should use systems of equations that are first order both in space and in time, since the second order in space and first order in time

scheme proved to be problematic. Thus, we proceed to do a first order reduction of the wave equation by defining $\Pi \equiv -\partial_T \psi$, obtaining

$$\begin{cases} \partial_T \psi = -\Pi \\ \partial_T \Pi = -\partial_{\underline{i}} \partial^{\underline{i}} \psi \end{cases} . \tag{13}$$

We can add an additional constraint $C_{\underline{i}} = \partial_{\underline{i}} \psi - \Phi_{\underline{i}} \overset{!}{=} 0$ to our system of equations, to which small violations could be allowed. Using the time derivative of this constraint as an evolution equation for Φ and expressing the small violation of this constraint as $\gamma_2 C_{\underline{i}}$, where γ_2 is a small parameter corresponding to the allowed violation, we get

$$\begin{cases} \partial_T \psi = -\Pi \\ \partial_T \Phi = -\partial_X \Pi + \gamma_2 \, \partial_X \psi - \gamma_2 \, \Phi \\ \partial_T \Pi = -\partial_X \Phi \end{cases} . \tag{14}$$

We then proceed to make a coordinate change from inertial Minkowski coordinates to hyperboloidal coordinates. Addicionally, even though we could allow for small violations of our constraint, we will not. Thus, we set $\gamma_2 = 0$, obtaining the final form of our system of equations:

$$\begin{cases} \partial_t \psi = -\Pi \\ \partial_t \Phi = \mathcal{A} \, \left(H' \, \partial_x \Phi + \partial_x \Pi \right) \\ \partial_t \Pi = \mathcal{A} \, \left(H' \, \partial_x \Pi + \partial_x \Phi \right) \end{cases} , \tag{15}$$

where we defined $\mathcal{A}(x) = \frac{\Omega^2(x)}{L(x)(H'^2(x)-1)}$, and dropped the explicit dependences on x to simplify the notation.

We can now solve this system of equations using the aforementioned code, using truncation error matching for the derivatives on the boundaries and turning off the artificial dissipation on those points. Using that framework and giving the initial conditions

$$\psi(0,x) = A \, e^{-C \, x^2/2} \, , \quad \Phi(0,x) = -A \, C \, x \, \frac{\Omega^2(x)}{L(x)} \, e^{-C \, x^2/2} \quad \text{and} \quad \Pi(0,x) = 0 \, , \tag{16}$$

with $A = 1.0$ and $C = 100$, we obtain the evolution present in figure 3. In that evolution, it is noticeable that after the wave leaves the grid, we are left with a permanent negative displacement on our field. Even though this result is counterintuitive, it was proven in [] to be correct.

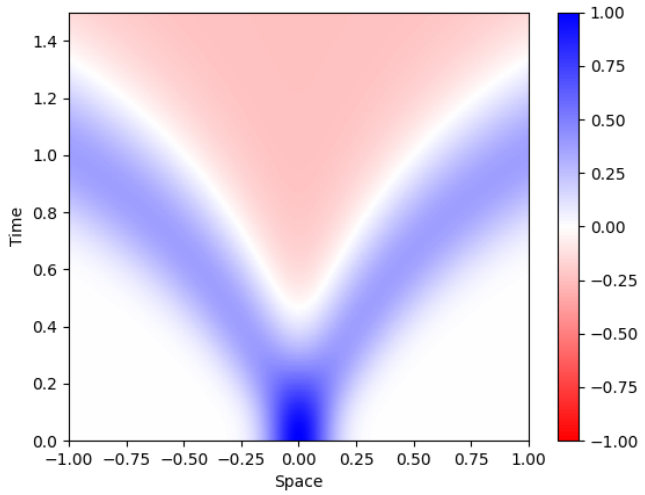

FIGURE 3: Evolution of the wave equation in 1+1 dimensions using hyperboloidal coordinates with the initial conditions given in equation (16).

Doing a norm convergence test (using the L^2 norm), we obtain a clean second order convergence during the whole evolution, as can be seen for ψ in the left of figure 4. We can also see that these results stay promising up until $\mathscr{I}$ through the pointwise convergence at that point, represented in the right of figure 4.

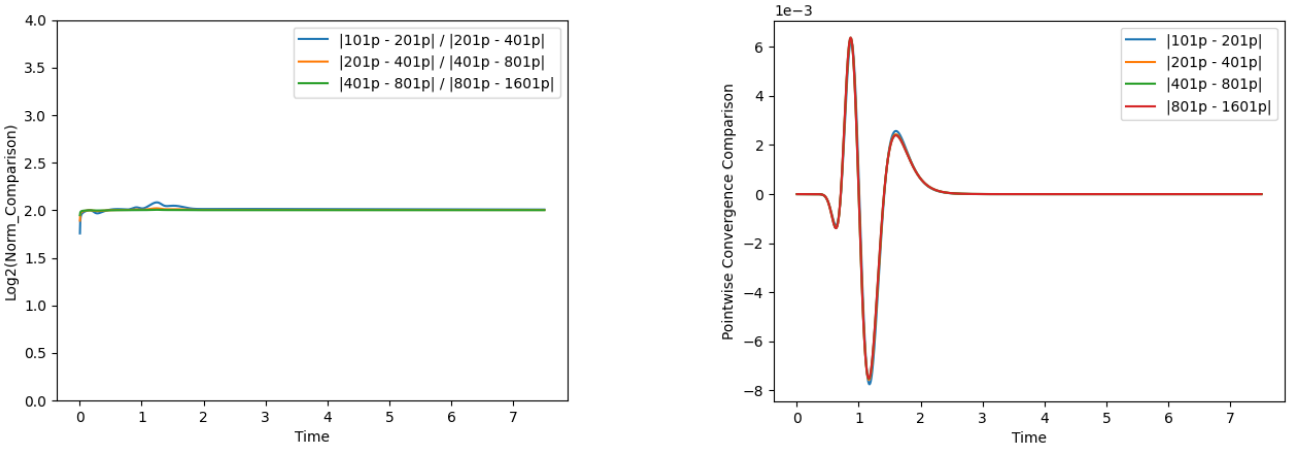

FIGURE 4: Convergence tests of the obtained evolutions for the wave equation in 1+1 dimensions using hyperboloidal coordinates. On the left, we have the L^2 norm convergence, and on the right, we have the pointwise convergence at $\mathscr{I}$.

3 Wave Equation in 3+1 Dimensions With Spherical Symmetry

Now, let us consider the wave equation in 3+1 dimensions with spherical symmetry

$$\Box\psi \equiv -\partial_T^2\psi + \frac{1}{R^2}\partial_R\left(R^2\partial_R\psi\right) = 0\,. \tag{17}$$

Since ψ is a solution to this equation, it will decay at a rate of $1/R$, which is a problem because we want to know how our field behaves at $\mathscr{I}$. Thus, we need to renormalize this field in such a way that it does not vanish at infinity. With this in mind, let us define a new field Ψ such that

$$\Psi \equiv \chi\,\psi\,,$$

where we will take $\chi = \sqrt{1+R^2}$.

Applying that transformation to the wave equation, it becomes

$$\partial_T^2\Psi = \partial_R^2\Psi + \frac{2}{R(R^2+1)}\partial_R\Psi - \frac{3}{(R^2+1)^2}\Psi\,, \tag{18}$$

to which we can apply a first order reduction, obtaining

$$\begin{cases} \partial_T\Psi = -\Pi \\ \partial_T\Phi = -\partial_R\Pi + \gamma_2\partial_R\Psi - \gamma_2\Phi \\ \partial_T\Pi = -\partial_R\Phi - \frac{2}{R(R^2+1)}\Phi + \frac{3}{(R^2+1)^2}\Psi \end{cases}. \tag{19}$$

Doing a coordinate change from inertial Minkowski coordinates to hyperboloidal coordinates and setting $\gamma_2 = 0$ as we did previously, we get

$$\begin{cases} \partial_T \Psi = -\Pi \\ \partial_T \Phi = \mathcal{B}\left((r^2+\Omega^2)^2\left(H'\partial_r\Phi + \partial_r\Pi\right) + H'L\Omega\left(2r\Phi - 3\Omega\Psi + 2r^{-1}\Omega^2\Phi\right)\right) \\ \partial_T \Pi = \mathcal{B}\left((r^2+\Omega^2)^2\left(\partial_r\Phi + H'\partial_r\Pi\right) + L\Omega\left(2r\Phi - 3\Omega\Psi + 2r^{-1}\Omega^2\Phi\right)\right) \end{cases}, \tag{20}$$

where we defined $\mathcal{B} = \frac{\Omega^2}{L(H'^2-1)(r^2+\Omega^2)^2}$.

We can see that in our evolution equations for Φ and for Π, we have a term that is formally singular, to which we will need to apply the Evans method. For that, we rewrite those evolution equations, obtaining

$$\begin{cases} \partial_T \Psi = -\Pi \\ \partial_T \Phi = \mathcal{B}\left((r^2+\Omega^2)^2\left(H'\partial_r\Phi + \partial_r\Pi\right) + H'L\Omega\left(2r\Phi - 3\Omega\Psi - \Omega^2\partial_r\Phi\right) + H'L\Omega^3\left(\partial_r\Phi + 2r^{-1}\Phi\right)\right) \\ \partial_T \Pi = \mathcal{B}\left((r^2+\Omega^2)^2\left(\partial_r\Phi + H'\partial_r\Pi\right) + L\Omega\left(2r\Phi - 3\Omega\Psi - \Omega^2\partial_r\Phi\right) + L\Omega^3\left(\partial_r\Phi + 2r^{-1}\Phi\right)\right) \end{cases}, \tag{21}$$

where it is easy to see that we can apply the Evans method to the last terms in parenthesis.

Imposing the parity of each field at the origin and doing extrapolation at $\mathscr{I}$ (instead of truncation error matching that we used before) as our boundary conditions and using the initial data

$$\psi(0,r) = A\, e^{-C\,r^2/2}\,, \quad \Phi(0,r) = -A\,C\,r\,\frac{\Omega^2(r)}{L(r)}\,e^{-C\,r^2/2} \quad \text{and} \quad \Pi(0,r) = 0\,, \tag{22}$$

with $A = 1.0$ and $C = 100$, we obtain the evolution represented in figure 5.

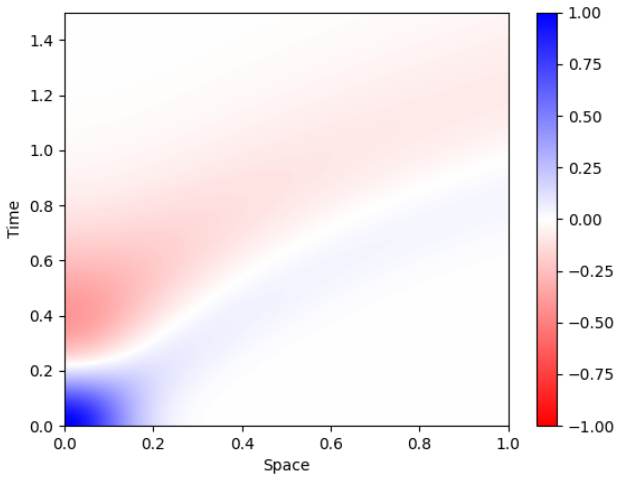

FIGURE 5: Evolution of the wave equation in 3+1 dimensions with spherical symmetry using hyperboloidal coordinates with the initial conditions given in equation (16).

Similarly to before, we obtain a clean second order convergence during the whole evolution, as can be seen for ψ in the left of figure 6. Addicionally, we still have very good pointwise convergence at $\mathscr{I}$, as can be seen in the right of figure 6. Despite the fact that these results are already very good, they could be further improved by doing truncation error matching at the outer boundary instead of the extrapolation that was used.

4 Cubic Wave Equation in 3+1 Dimensions With Spherical Symmetry

5 Conclusions

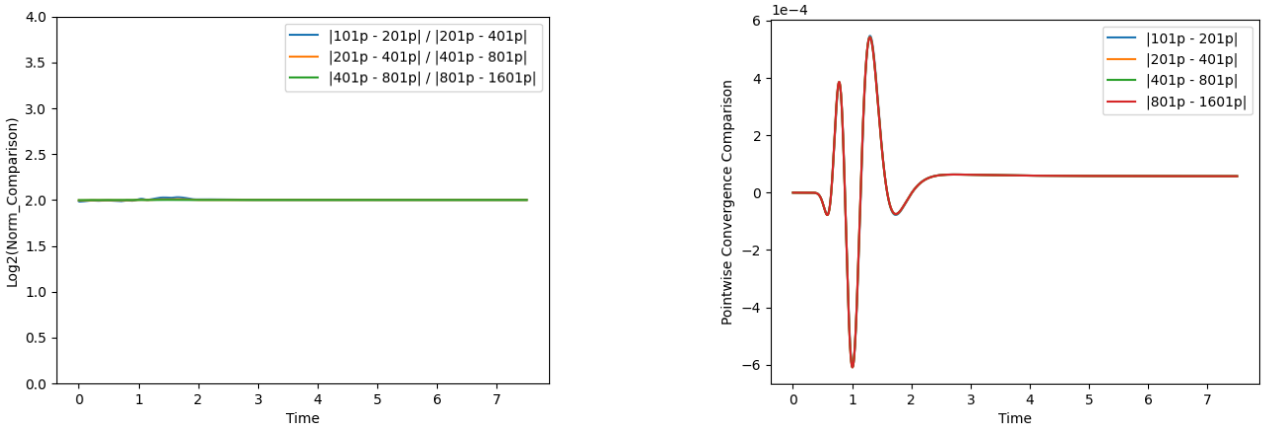

FIGURE 6: Convergence tests of the obtained evolutions for the wave equation in 3+1 dimensions with spherical symmetry using hyperboloidal coordinates. On the left, we have the L^2 norm convergence, and on the right, we have the pointwise convergence at $\mathscr{I}$.